

Ergodicity Test of the Eddy covariance technique

Jinbei CHEN¹ Yinqiao HU² Ye YU Shihua LÜ

Key Laboratory of Land Surface Processes and Climate Change in Cold and Arid Regions; Cold and Arid Regions Environment and Engineering Institute, Chinese Academy of Sciences, Lanzhou 730000, P R China.

Pingliang Land Surface Process & Severe Weather Research Station, Chinese Academy of Science, Pingliang 744015, P R China.

1 E-mail: chenjinbei@lzb.ac.cn

2 Corresponding author: hyq@ns.lzb.ac.cn

Abstract

The ergodic hypothesis is a basic hypothesis typically invoked in atmospheric surface layer (ASL) experiments. The ergodic theorem of stationary random processes is introduced to analyze and verify the ergodicity of atmospheric turbulence measured using the eddy covariance technique with two sets of field observational data. The results show that eddies of atmospheric turbulence, of which the scale is smaller than the scale of the atmospheric boundary layer (ABL), i.e., the spatial scale is less than 1,000 m and temporal scale is shorter than 10 min, can effectively satisfy the ergodic theorems. Under these restrictions, a finite time average can be used as a substitute for the ensemble average of atmospheric turbulence. Whereas, eddies that are larger than ABL's scale cannot satisfy the mean ergodic theorem. Consequently, when a finite time average is used to substitute for the ensemble average, the eddy correction method incurs large errors due to the loss of low frequency information associated with larger eddies. A multi-station observation is compared with a single-station, and then the scope that satisfies the ergodic theorem is extended from smaller than the ABL's scale about 1000 m to greater than that about 2000 m. Therefore, the calculation of averages, variances and fluxes of turbulence can effectively satisfy the ergodic assumption, and the results are more approximate to the actual values. Regardless of vertical velocity or temperature, the variance of eddies at different scales follow Monin-Obukhov Similarity Theory (MOST) better if the ergodic theorem can be satisfied, if not it deviates from MOST. The ergodicity exploration of atmospheric turbulence is doubtlessly helpful in understanding the issues in atmospheric turbulent observations, and provides a theoretical basis for overcoming related difficulties.

Keywords: Ergodic hypothesis; eddy covariance technique; Monin-Obukhov

35 similarity theory (MOST); atmospheric surface layer (ASL); high-pass filtering

36

37 **1 Introduction**

38 The basic principle of the average of a turbulence measurement is based on ensembles
39 averaged over space, time and state. However, it is impossible to make an actual
40 turbulence measurement with enough observational instruments in space for sufficient
41 time to obtain all states of turbulent eddies to achieve the goal of an ensemble average.
42 Therefore, based on the ergodic hypothesis, the time average of one spatial point,
43 ~~where is long enough for observation,~~ is used as a substitute for the ensemble average
44 for temporally steady and spatially homogeneous surfaces (Stull 1988; Wyngaard
45 2010; Aubinet 2012). The ergodic hypothesis is a basic assumption in turbulence
46 experiments in the atmospheric boundary layer (ABL) and atmospheric surface layer
47 (ASL). Stationarity, homogeneity, and ergodicity are routinely used to link ensemble
48 statistics (mean and higher-order moments) of field experiments in the ABL. Many
49 authors habitually refer to the ergodicity assumption with descriptions such as “when
50 satisfying ergodic hypothesis.....” or “something indicates that ergodic hypothesis is
51 satisfied”. The success of Monin-Obukhov Similarity Theory (MOST) for unstable
52 and near-neutral conditions is just evidence of the validity of the ergodic hypothesis in
53 the ASL, ~~which~~ ergodicity is a necessary condition for the success of MOST, it does
54 not prove ergodicity (~~Katul and Poggi 2004~~). The success of MOST under the
55 conditions of stationary and homogeneity implies that they are the important
56 conditions of ASL ergodicity. Therefore, many ABL experiments focus on seeking
57 ideal homogeneous surface. Test procedures are widely applied to establish
58 stationarity (Foken and Wichura 1996; Vickers and Mahrt 1997). Katul and Hsieh-
59 (2004) qualitatively analyzed the ergodicity problem in atmospheric turbulence, and
60 believed that it is common for the neutral and unstable ASL to ~~reach~~ ergodicity, while
61 it is difficult to reach ergodicity in the stable ASL. Eichinger et al. (2001) indicate that
62 LIDAR (Light Detection and Ranging) technique opens up new possibilities for
63 atmospheric measurements and analysis by providing spatial and temporal
64 atmospheric information with simultaneous high-resolution. The stationarity and
65 ergodicity can be tested for such ensembles of experiments. Recent advances in
66 LIDAR measurements offers a promising first step for direct evaluation of such
67 hypotheses for ASL flows (Higgins et al., 2013). Higgins et al. (2013) applied LIDAR

68 of water vapor concentration to investigate the ergodic hypothesis of atmospheric
69 turbulence for the first time. It is clear all the same that there is a need to reevaluate
70 turbulence measurement technology, to test the ergodicity of atmospheric turbulence
71 quantitatively by means of observation experiments.

72 The ergodic hypothesis was first proposed by Boltzmann (Boltzmann 1871; Uffink
73 2004) in his study of the ensemble theory of statistical dynamics. He argued that a
74 trajectory traverses *all* points on the energy hypersurface after a certain amount of
75 time. At the beginning of 20th century, the Ehrenfest couple (Ehrenfest and
76 Ehrenfest-Afanassjewa 1959; Uffink 2004) proposed a quasi-ergodic hypothesis and
77 changed the term “traverses *all* points” in the aforesaid ergodic hypothesis to “passes
78 arbitrarily close to every point”. The basic points of ergodic hypothesis or
79 quasi-ergodic hypothesis recognize that the macroscopic property of a system in the
80 equilibrium state is the average of microcosmic quantity in a certain amount of time.
81 Nevertheless, the ergodic hypothesis or quasi-ergodic hypothesis were never proven
82 theoretically. The proof of the ergodic hypothesis in physics aroused the interest of
83 mathematicians. The famous mathematician, Neumann et al. (1932) first theoretically
84 proved the ergodic theorem in topological space (Birkhoff 1931, Krengel 1985).
85 Afterward, a banauic ergodic theorem of stationary random processes was proved to
86 provide the necessary and sufficient conditions for the ergodicity of stationary random
87 processes. Mattingly (2003) reviewed research progress on ergodicity for
88 stochastically force Navier-Stokes equation, and Galanti and Tsinober (2004), and
89 Lennaert et al. (2006) solved the Navier-Stokes equation by numerical simulation to
90 prove that turbulence which is temporally steady and spatially homogeneous is
91 ergodic. However, Galanti and Tsinober (2004) also indicated that such partially
92 turbulent flows acting as mixed layer, wake flow, jet flow, flow around the boundary
93 layer may be non-ergodic turbulence.

94 Obviously, the advances of research on ergodicity in the mathematics and physics
95 have led the way for the atmospheric sciences. We try first to introduce the ergodic
96 theorem of stationary random processes to atmospheric turbulence in the ASL in this
97 paper. The ergodicity of different scale eddies of atmospheric turbulence is directly
98 analyzed and verified quantitatively on the basis of field observations obtained using
99 eddy covariance technique.

100 **2 Theories and methods**

101 2.1 Ergodic theorems of stationary random processes

102 Stationary random processes are processes which will not vary with time, i.e., for
103 observed quantity A , its function of space x_i and time t_i satisfies the following
104 condition:

$$105 A(x_1, x_2, \dots, x_n; t_1, t_2, \dots, t_n) = A(x_1, x_2, \dots, x_n; t_1 + \tau, t_2 + \tau, \dots, t_n + \tau), \quad (1)$$

106 where τ is a time period, defined as the relaxation time.

107 The mean μ_A of a random variable A and autocorrelation function $R_A(\tau)$ are
108 respectively defined as following:

$$109 \mu_A = \lim_{T \rightarrow +\infty} \frac{1}{T} \int_0^T A(t) dt, \quad (2)$$

$$110 R_A(\tau) = \lim_{T \rightarrow +\infty} \frac{1}{T} \int_0^T A(t) A(t + \tau) dt. \quad (3)$$

111 The autocorrelation function $R_A(\tau)$ is a temporal second-order moment. In the case of
112 $\tau=0$, the autocorrelation function $R_A(\tau)$ is the variance of random variable. A necessary
113 and sufficient condition for a stationary random processes to satisfy the mean
114 ergodicity are the mean ergodic function $Ero(A)$ to zero (Papoulis and Pillai 1991), as
115 shown below:

$$116 Ero(A) = \lim_{T \rightarrow \infty} \frac{1}{T} \int_0^{2T} \left(1 - \frac{\tau}{2T}\right) [R_A(\tau) - \mu_A^2] d\tau = 0. \quad (4)$$

117 The mean ergodic function $Ero(A)$ is a time integral of variation between the
118 autocorrelation function $R_A(\tau)$ of variable A and its mean square, μ_A^2 . If the mean
119 ergodic function $Ero(A)$ converges to zero, then the stationary random processes will
120 be ergodic. In other words, if the autocorrelation function $R_A(\tau)$ of variable A
121 converges to its mean square, μ_A^2 , the stationary random processes are mean ergodic.

122 The Eq. (4) is namely mean ergodic theorem to be called as well as ergodic theorem
123 of the *weakly* stationary processes in the mathematics. For discrete variables, Eq. (4)
124 can be rewritten as following:

$$125 Ero(A) = \lim_{n \rightarrow \infty} \sum_{i=0}^n \left(1 - \frac{\tau_i}{n}\right) [R_A(\tau_i) - \mu_A^2] = 0. \quad (5)$$

126 Eq. (5) is mean ergodic theorem of the discrete variable. Hence, Eqs. (4) or (5) can be
127 used as a criterion to judge the mean ergodicity.

128 For the stationary random processes, the necessary and sufficient condition

129 satisfying the autocorrelation ergodicity are the autocorrelation ergodic function $\text{Er}(A)$
 130 to zero:

$$131 \quad \text{Er}(A) = \lim_{T \rightarrow \infty} \frac{1}{T} \int_0^{2T} \left(1 - \frac{\tau'}{2T}\right) [B(\tau') - |R_A(\tau)|^2] d\tau' = 0; \quad (6a)$$

$$132 \quad B(\tau') = E \left\{ A(t + \tau + \tau') A(t + \tau) [A(t + \tau) A(t)] \right\}. \quad (6b)$$

133 Where τ' is a differential variable for entire relaxation times, and that $B(\tau')$ is temporal
 134 fourth-order moment of variable A . The autocorrelation ergodic function $\text{Er}(A)$ is a
 135 time integral of variation between the temporal fourth-order moment $B(\tau')$ of variable
 136 A and its autocorrelation function square, $|R_A(\tau)|^2$. If the autocorrelation ergodic
 137 function $\text{Er}(A)$ converges to zero, then the stationary random processes will be of
 138 autocorrelation ergodicity, and thus the autocorrelation ergodicity means that the
 139 fourth-order moment of variable of stationary random processes will converge to
 140 square of its autocorrelation function $R_A(\tau)$. The Eq. (6a) is namely autocorrelation
 141 ergodic theorem to be called as well as ergodic theorem of the *strongly* stationary
 142 processes in the mathematics. The autocorrelation ergodic function of corresponding
 143 discrete variable can be determined as following:

$$144 \quad \text{Er}(A) = \lim_{n \rightarrow \infty} \sum_{i=0}^n \left(1 - \frac{\tau'_i}{n}\right) [B(\tau'_i) - |R_A(\tau_j)|^2] = 0, \quad (7a)$$

$$145 \quad B(\tau'_i) = E \left\{ \sum_{j=0}^n A(t + \tau_j + \tau'_i) A(t + \tau'_i) [A(t + \tau_j) A(t)] \right\}. \quad (7b)$$

146 Eq. (7a) is autocorrelation ergodic theorem of the discrete variable. Hence, Eqs. (6a)
 147 or (7a) can also be used as a criterion to judge the autocorrelation ergodicity.

148 The stationary random processes conform to the criterion, Eqs. (4) or (5), then they
 149 satisfy the mean ergodic theorem, or are intituled as the mean ergodicity; the
 150 stationary random processes conform to the criterion, Eqs. (6a) or (7a), then they
 151 satisfy the autocorrelation ergodic theorem, or are intituled as the autocorrelation
 152 ergodicity. If the stationary random processes are only of mean ergodicity, they are
 153 strict ergodic or narrow ergodic. If the stationary random processes are of both the
 154 mean ergodicity and autocorrelation ergodicity, they are wide ergodic stationary
 155 random processes. It is thus clear that the ergodic random processes are stationary, but
 156 the stationary processes may not be ergodic.

157 With respect to the random process theory, when a mean or high-order moment
158 function is calculated, a large amount of repeated observations requires to acquire a
159 sample function $A_k(t)$. If the stationary random processes satisfy the ergodic condition,
160 then time average of a sample on the whole time shaft can be used to substitute for the
161 ensemble average. The Eqs. (4), (5), (6a) and (7a) can be used as the criterion to judge
162 whether or not satisfying the mean and autocorrelation ergodicity. The ergodic
163 random processes must be the stationary random processes to be defined as Eq. (1),
164 and thus are stationary in relaxation time τ . If the condition such as Eqs (4) or (5) of
165 the mean ergodicity is satisfied, then a time average in finite relaxation time τ can be
166 used to substitute for infinite time average to calculate the mean Eq. (2) of random
167 variable; similarly, the finite time average can be used for substitution to calculate the
168 covariance or variance of random variable, Eq. (3), if the condition such as Eqs. (6a)
169 or (7a) of autocorrelation ergodicity is satisfied. In a similar manner, basic principle of
170 the average of the atmospheric turbulence is the ensemble average of space, time and
171 state, and it is necessary to carry through mass observations for a long period of time
172 in the whole space. This is not only a costly observation, even is hardly feasible. If the
173 turbulence satisfies the ergodic condition, then a time average in relaxation time τ by
174 multi-station observation, even single-station observation, can substitute for the
175 ensemble average. In fact, precondition to estimate turbulent characteristic quantities
176 and fluxes in the ABL by the eddy covariance technique is that the turbulence satisfies
177 the ergodic condition. Therefore, conditions such as Eqs. (4), (5), (6a) and (7a) will
178 also be the criterion for testing the authenticity of results observed by the eddy
179 covariance technique.

180 **2.2 Band-pass filtering**

181 The scope of spatial and temporal scale of the atmospheric turbulence, which is from
182 the dissipation range, inertial sub-range to the energy range, and further the turbulent
183 large eddy, is extremely broad (Stull 1988). In such wide spatial and temporal scope,
184 the turbulent eddies include the isotropic 3-D eddy structure of high frequency
185 turbulence and orderly coherent structure of low frequency turbulence (Li et al. 2002).
186 These eddies of different scale are also each other different in terms of their spatial
187 structure and physical properties, and even their transport characteristics are not all
188 same. It is thus reasonable that eddies with different characteristics are separated,
189 processed and studied using different methods (Zuo et al. 2012). A major goal of our

190 study is to understand what type of eddy in the scale can satisfy the ergodic condition.
 191 Another goal is that the time averaging of signals measured by a single station
 192 determines accurately turbulent characteristic quantities. In order to study the
 193 ergodicity of different scale eddies, Fourier transform is used as a band-pass filtering
 194 to distinguish different scale eddy. That is to say, we set the Fourier transform
 195 coefficient of the part of frequencies, which does not need, as zero, and then acquire
 196 the signals after filtering by means of Fourier inverse transformation. The specific
 197 formulae are shown below:

$$198 \quad F_A(n) = \frac{1}{N} \sum_{k=0}^{N-1} A(k) \cos\left(\frac{2\pi nk}{N}\right) - \frac{i}{N} \sum_{k=0}^{N-1} A(k) \sin\left(\frac{2\pi nk}{N}\right), \quad (8)$$

$$199 \quad A(k) = \sum_{n=a}^{N-1} F_A(n) \cos\left(\frac{2\pi nk}{N}\right) + i^2 \sum_{n=a}^{N-1} F_A(n) \sin\left(\frac{2\pi nk}{N}\right). \quad (9)$$

200 In Eqs. (8) and (9), $F_A(n)$ and $A(k)$ are respectively the Fourier transformation and
 201 Fourier inverse transformation including N data points from $k=0$ to $k=N-1$, and n is the
 202 cycle index of the observation time range. The high-pass filtering can cut off the low
 203 frequency signals of turbulence to obtain the high frequency signals. An aliasing of
 204 half high frequency turbulence after the Fourier transformation is unavoidable. At the
 205 same time, the correction for high frequency response will compensate for that loss. In
 206 order to acquire purely the high frequency signals in filtering processes, we take
 207 results of the band-pass filtering from $n=j$ to $n=N-j$ as the high frequency signals. This
 208 is referred to as j time filtering in this paper. Finally, the ergodicity of different scale
 209 eddies is analyzed using the Eqs. (4)-(7).

210 **2.3 MOS of turbulent variance**

211 The characteristics of the relations of Monin-Obukhov Similarity (MOS) for the
 212 variance of different scale eddies are analyzed and compared to test feasibility of the
 213 MOS's relation for ergodic and non-ergodic turbulence. The problems of eddy
 214 covariance technique in the turbulence observation in ASL are further explored on the
 215 basis of studying on the ergodicity and MOS's relations of the variance of different
 216 scale eddies in order to provide an experimental basis for utilizing MOST and
 217 developing the turbulence theory of ABL with complex underlying surfaces.

218 The MOS's relations of turbulent variance can be regarded as an effective
 219 instrumentality to verify whether or not the turbulent flow field is steady and
 220 homogeneous (Foken et al. 2004). Under ideal conditions, the local MOS's relations

221 of the variance of wind velocity, temperature and other factors can be expressed as
 222 following:

$$223 \quad \sigma_i/u_* = \phi_i(z/L), \quad (i = u, v, w), \quad (10)$$

$$224 \quad \sigma_s/|s_*| = \phi_s(z/L), \quad (s = \theta, q). \quad (11)$$

225 where σ is turbulent variance; corner mark i is wind velocity u , v or w ; s stands for
 226 scalar, such as potential temperature θ and humidity q ; u_* is friction velocity and

227 defined as $u_* = \left(\overline{u'w'^2} + \overline{v'w'^2} \right)^{1/4}$; s_* is the turbulent characteristic quantity related to

228 scalar defined as $s_* = -\overline{w's'}/u_*$; and that M-O length L is defined as (Hill 1989):

$$229 \quad L = u_*^2 \theta / [\kappa g (\theta_* + 0.61 \theta q_* / \rho_d)], \quad (12)$$

230 where ρ_d is dry air density .

231 A large number of research results show that, in the case of unstable stratification,
 232 $\phi_i(z/L)$ and $\phi_s(z/L)$ can be expressed in the following forms (Panofsky et al. 1977;
 233 Padro 1993; Katul et al. 1999):

$$234 \quad \phi_i(z/L) = c_1 (1 - c_2 z/L)^{1/3}; \quad (13)$$

$$235 \quad \phi_s(z/L) = \alpha_s (1 - \beta_s z/L)^{-1/3}. \quad (14)$$

236 where c_1 , c_2 , α and β are coefficients to be determined by the field observation. In the
 237 case of stable stratification, $\phi_s(z/L)$ is approximate to a constant and $\phi_i(z/L)$ is
 238 still the 1/3 function of z/L . The turbulent characteristics of eddies in different
 239 temporal and spatial scale are analyzed and compared with the mean and
 240 autocorrelation ergodic theorems, to test feasibility of the MOS's relations under the
 241 condition of the ergodic and non-ergodic turbulence.

242 3 The sources and processing of data

243 In this study, the first turbulence data set that were measured by the eddy covariance
 244 technique under the homogeneous surface in Nagqu Station of Plateau Climate and
 245 Environment (NSPCE), Chinese Academy of Sciences (CAS) is used. The data set in
 246 NSPCE/CAS includes the data that measured by 3-D sonic anemometer and
 247 thermometer (CSAT3) with 10 Hz as well as infrared gas analyzer (Li7500) in ASL
 248 from 23 July 2011 to 13 September 2011. In addition, the second turbulence data set

249 of CASES-99 (Poulos et al. 2002; Chang and Huynh. 2002) is used to verify the
250 ergodicity of turbulence observed by multi-station. The CASES-99 has seven
251 observation points. The sub-towers, sn1, sn2 and sn3 are located 100 m away from the
252 central tower, the sub-tower sn4 is 280 m away, and sub-towers sn5 and sn6 are
253 located 300 m away. The data in the central tower of CASES-99 include that
254 measured by sonic anemometer and thermometer (CSAT3) with 20 Hz and the
255 infrared gas analyzer (Li7500) at 10m on tower with 55 m height in ASL. And other
256 data in the sub-towers of CASES-99 include that measured by 3-D sonic anemometer
257 (ATI) and Li7500 at 10 m height on six sub-towers surrounding the central tower. The
258 analyzed results with two data sets for completely different purposes are compared to
259 test universality of the research results.

260 The geographic coordinate of NSPCE/CAS is 31.37°N, 91.90°E, and its altitude is
261 4509 m a.s.l. The observation station is built on flat and wide area except for a hill of
262 about 200 m at 2 km distance in the north, and floor area is 8000m². The ground
263 surface is mainly composed of sandy soil mixed with sparse fine stones, and a plateau
264 meadow with vegetation of 10-20 cm. The roughness length and displacement height
265 of underlying surface of NSPCE's meadow is respectively determined to 0.009 m and
266 0.03 m. CASES-99 is located in prairie of Kansas US. The geographic coordinate of
267 CASES-99's central tower is 37.65°N, 96.74°W. The observation field is flat and
268 growth grasses about 20-50 cm during the observation period, while the roughness
269 length and displacement height of CASES-99's underlying surface is 0.012 m and
270 0.06 m, respectively (Martano 2000).

271 The data are selected to study the ergodicity observed turbulent eddies in ABL.
272 Firstly the inaccurate data caused by spike are deleted before data analysis.
273 Subsequently, the data are divides into continuous sections of 5-hour, and the high
274 frequency signals of 1-hour are obtained applying filtering of the Eqs. (8) and (9) for
275 each 5-hour data. In order to delete further the abnormal inaccurate data, the data are
276 divides once again into 12 continuous fragments of 5-min in 1-hour. The variances of
277 velocity and temperature are calculated and compared each other for the fragments.
278 The data that deviation is less than $\pm 15\%$ including an instrumental error
279 about $\pm 5\%$ are selected. Moreover, temperature of the ultrasonic pulse signals is
280 converted to absolute temperature (Schotanus et al. 1983; Kaimal and Gaynor 1991).
281 Then all data without spike for 25 days are done the coordinate rotation using the

282 plane fitting method to improve the levelness of instrument installation (Wilczak
283 2001). The trend correction (McMillen 1988; Moore 1986) is used to exclude the
284 influence of low-frequency trend effect caused by the diurnal variations and weather
285 processes. The Webb correction (Webb et al. 1980) is a component of surface energy
286 balance in physical nature, but not the component of turbulent eddy. However, this
287 study is to analyze the ergodicity of turbulent eddies. According to our preliminary
288 analysis about the ergodicity of turbulent eddies, such correction may cause the
289 unreasonable deviation from the prediction with Eq. (14). We thus do not perform the
290 Webb correction in our research on the ergodicity.

291 **4. Result analysis**

292 Applying the two data sets from NSPCE and CASES-99, the ergodicity of different
293 temporal scale eddies is tested. Here as an example, we select representative data
294 measured at level of 3.08m in NSPCE during three time frames, namely 3:00-4:00,
295 7:00-8:00 and 13:00-14:00 China Standard Time (CST) on 25 August in clear weather
296 to test and demonstrate the ergodicity of different temporal scale eddies. These three
297 time frames can represent three situations, i.e. the nocturnal stable boundary layer,
298 early neutral boundary layer and midday convective boundary layer.

299 The Eqs. (8) and (9) are used to perform band-pass filtering from $n=j$ to $n=N-j$ to
300 acquire the signals of eddies corresponding temporal scale. The turbulence
301 characteristics and ergodicity of eddies in the different temporal scale including 2 min,
302 3 min, 5 min, 10 min, 30 min and 60 min are studied using above processed data for
303 three time frames.

304 **4.1 M-O eddy local stability and M-O stratification stability**

305 The M-O stratification stability parameter z/L describe a whole characteristic between
306 the mechanical and buoyancy effect of ASL's turbulence, but this study will
307 decompose the turbulence into different scale eddies. Considering that the property of
308 different scale eddies of the atmospheric turbulence varies with the atmospheric
309 stability parameter z/L , a M-O eddy local stability that is limited in the certain scale
310 range of eddies is defined as z/L_c , so as to analyze relation between the stratification
311 stability and ergodicity of the different scale eddies for the wind velocity, temperature
312 and other factors. It is worth noting that the M-O eddy local stability, z/L_c , is different
313 from the M-O stratification stability, z/L .

314 As an example, the eddy local stability z/L_c in the different temporal scales of the

315 three time frames from the nighttime to the daytime is as shown in Table 1. The
316 results show that the eddy local stability z/L_c below 2 min in temporal scale during the
317 nighttime time frame at time 3:00-4:00 AM(CST) is 0.59, thus it is stable stratification.
318 But as the eddy temporal scale gradually increases from 3 min, 5 min and 10 min to
319 60 min, the eddy local stability, z/L_c , gradually decreases to 0.31 and 0.28. Even
320 starting from 10 min in the temporal scale, the eddy local stability decreases from
321 -0.01 to -0.07. It seems that the eddy local stability gradually varies from stable to
322 unstable as the eddy temporal scale increases. During the morning time frame at
323 7:00-8:00 AM (CST), the eddy local stability z/L_c from 2 min to 60 min in the
324 temporal scale eventually decreases from 0.52, 0.38, 0.16 and 0.15 to -0.43 in 30 min
325 and a minimum of -1.29 in 60 min. It means that eddies in the temporal scales of 30
326 min and 60 min have high local instability. However, during the midday time frame at
327 14:00-15:00 PM (CST), eddies in the temporal scales from 2 min to 60 min are
328 unstable. Now $-z/L_c$ is defined as eddy local instability. As the eddy scale increases,
329 the eddy local instability in the scales from 2 min to 3 min also increases, and its
330 value reaches a maximum of 0.44 as the eddy scale is 5 min. But as the eddy scale
331 increases continuously, the eddy local instability is reduced.

332 The M-O eddy local stability is not entirely the same as the M-O stratification
333 stability of ABL in the physical significance. The M-O stratification stability of ABL
334 indicates the overall effect of atmospheric stratification of the ABL on the stability
335 including all eddies in integral boundary layer. The M-O stratification stability z/L is
336 stable 0.02 at 3:00-4:00 AM (CST) for no filtering data to include the whole turbulent
337 signals, but unstable -0.004 and -0.54 at 7:00-8:00 and 13:00-14:00 PM (CST),
338 respectively. However the eddy local stability is only a local effect of atmospheric
339 stratification on the stability of eddies in a certain scale. As the eddy scale increases,
340 the eddy local stability z/L_c will vary accordingly. The aforesaid results indicate that
341 the local stability of small-scale eddies is stable in the nocturnal stable boundary layer,
342 but it is possibly unstable for the large-scale eddies. As a result, a sink effect on the
343 small-scale eddies in the nocturnal stable boundary layer, but a positive buoyancy
344 effect on the large-scale eddies. However, in diurnal unstable boundary layer, the eddy
345 local instability of 3 min scale reaches a maximum, and then the instability gradually
346 decreases as the eddy scale increases. Therefore, eddies of 3 min scale hold maximum
347 buoyancy, but the eddy buoyancy decreases as the eddy scale increases continuously.

348 Nevertheless, the small-scale eddies are more stable than the large scale eddies in the
349 nocturnal stable boundary layer; the large-scale eddies are more stable than the small
350 scale eddies in the diurnal unstable and convective boundary layers. The above facts
351 signify that it is common that there exist mainly the small-scale eddies in the
352 nocturnal boundary layer with stable stratification. And it is also common that there
353 exist mainly the large-scale eddies in the diurnal convective boundary layer with
354 unstable stratification. Therefore, it can well understand that the small-scale eddies are
355 dominant in the nocturnal stable boundary layer, while the large-scale eddies are
356 dominant in the diurnal convective boundary layer.

357 **4.2 Verification of mean ergodic theorem of the eddies in different temporal scale**

358 In order to verify the mean ergodic theorem, we calculated the mean and
359 autocorrelation functions using Eq. (2) and Eq. (3), then calculated the variation of
360 mean ergodic function $Ero(A)$ using Eq. (5) of eddies in the different temporal scale
361 with relaxation time τ to be cut off with $\tau_{i=n}$. The mean ergodic functions, $Ero(A)$, of
362 vertical velocity, temperature and specific humidity of the different scale eddies are
363 calculated using data at level of 3.08m for three time frames at 3:00-4:00, 7:00-8:00
364 and 13:00-14:00 (CST) in NSPCE, as shown in Figs. 1-3 respectively. Since the
365 ergodic function varies within a large range, the ergodic functions are normalized
366 according to characteristic quantity of relevant variables ($A_* = u_*, |\theta_*|, |q_*|$). That is to
367 say, functions in all following figures are the dimensionless ergodic functions,
368 $Ero(A)/A_*$.

369 Comprehensive analyses of characteristics of the mean ergodicity of atmospheric
370 turbulence and relevant causes:

371 4.2.1 Verifying mean ergodic theorem of different scale eddies

372 According to the mean ergodic theorem, Eq. (4), the mean ergodic function $Ero(A)/A_*$
373 will converge to 0 if the time approaches infinite. This is only a theoretical result of
374 the stationary random processes. A practical mean ergodic function is calculated under
375 the condition of that relaxation time $\tau_{i=n}$ is cut off. If the mean ergodic function
376 $Ero(A)/A_*$ converges approximately to 0 in relaxation time $\tau_{i=n}$, it will be considered
377 that random variable A approximately satisfies the mean ergodic theorem. The mean
378 ergodic function deviates more from zero, the mean ergodicity will be of poor quality.
379 Consequently, we can judge approximately the mean ergodic theorem of different
380 scale eddies whether or not holds. Figs. 1-3 clearly show that, regardless of the

381 vertical velocity, temperature or humidity, the $Ero(A)/A^*$ of eddies below 10 min in the
382 temporal scale will swing around zero within a small range; thus we can conclude that
383 the mean ergodic function $Ero(A)/A^*$ of eddies below 10 min in the temporal scale
384 converges to zero to satisfy effectively the condition of mean ergodic theorem. For
385 eddies of 30 min and 60 min, which are larger scale, the mean ergodic function
386 $Ero(A)/A^*$ will deviate further from zero. In particular, the mean ergodic function
387 $Ero(A)/A^*$ of eddies of 30 min and 60 min for the temperature and humidity does not
388 converge, and even diverges. Above results show that the mean ergodic function of
389 eddies of 30 min and 60 min cannot converge to zero or cannot satisfy the condition
390 of mean ergodic theorem.

391 4.2.2 Comparison of the convergence of mean ergodic functions of vertical velocity, 392 temperature and humidity

393 As seen from the Figs. 1-3, dimensionless mean ergodic function of the vertical
394 velocity is compared with respective function of the temperature and humidity, it is
395 3-4 magnitudes less than those in the nocturnal stable boundary layer; 1-2 magnitudes
396 less than those in the early neutral boundary layer; and about 2 magnitudes less than
397 those in the midday convective boundary layer. For example, during nighttime time
398 frame at 3:00-4:00 PM (CST), the dimensionless mean ergodic function of vertical
399 velocity is 10^{-5} in magnitude, while respective magnitudes of function value of the
400 temperature and humidity are 10^{-1} and 10^{-2} ; during morning time frame at 7:00-8:00
401 AM (CAT), magnitude of mean ergodic function of the vertical velocity is 10^{-4} , while
402 the respective magnitudes of function value of the temperature and humidity are 10^{-2}
403 and 10^{-3} ; during midday time frame at 13:00-14:00 PM(CST), magnitude of mean
404 ergodic function of the vertical velocity is 10^{-4} , while the magnitudes of function
405 value of the temperature and humidity are both 10^{-2} . These results show that the
406 dimensionless mean ergodic function of vertical velocity converges to zero much
407 more easily than respective function value of the temperature and humidity, and that
408 the vertical velocity satisfies the condition of mean ergodic theorem to overmatch
409 more than the temperature and humidity.

410 4.2.3 Temporal scale and spatial scale of turbulent eddies

411 For wind velocity of $1-2 \text{ ms}^{-1}$, eddy spatial scale in the temporal scale 2 min is around
412 120-240 m, and eddy spatial scale in the temporal scale of 10 min is around 600-1200
413 m. The eddy spatial scale in the temporal scale of 2 min is equivalent to ASL's height,

414 and the eddy spatial scale in the temporal scale of 10 min is equivalent to ABL's
415 height. The eddy spatial scale within the temporal scales of 30-60 min is around
416 1800-3600 m, and this spatial scale clearly exceeds ABL's height to belong to scope
417 of the atmospheric local circulation. According to the stationary random processes
418 definition (1) and mean ergodic theorem, the stationary random processes must be
419 smooth in relaxation time τ . The eddies below temporal scale of 10 min, i.e., below
420 ABL's height, are the stationary random processes, and can effectively satisfy the
421 condition of mean ergodic theorem. However, eddies in the temporal scales of 30 min
422 and 60 min exceed ABL's height and do not satisfy the condition of mean ergodic
423 theorem, thus these eddies belong to the non-stationary random processes.

424 4.2.4 Turbulence ergodicity of all eddies in possible scales in ABL

425 To facilitate comparison, Fig. 4 shows the variation of mean ergodic function $Ero(A)$
426 of the vertical velocity (a), temperature (b) and specific humidity (c) before filtering
427 with relaxation time τ during midday time frame at 14:00-15:00 PM (CST) in
428 convective boundary layer. It is obvious that Fig. 4 is unfiltered mean ergodic
429 function of eddies in all possible scales in ABL. The Fig. 4 compares with Figs. 1c, 2c
430 and 3c, which are the mean ergodic function $Ero(A)/A^*$ of vertical velocity,
431 temperature and humidity after filtering during the midday time frame at 14:00-15:00
432 PM (CST). The result shows that the mean ergodic functions before filtering are
433 greater than that after filtering. As shown in Figs. 1c, 2c and 3c, magnitude for the
434 vertical velocity is 10^{-4} and magnitudes for the temperature and specific humidity are
435 both 10^{-2} . According to the Fig. 4, the magnitude of vertical velocity $Ero(A)/A^*$ is 10^{-3}
436 and the magnitudes of temperature and specific humidity are both 10^0 , therefore 1-2
437 magnitudes are almost decreased after filtering. Moreover, all trend upward deviating
438 from zero for vertical velocity and temperature and downward deviating from zero for
439 specific humidity. It is thus clear that, during the midday time frame at 14:00-15:00
440 PM (CST). when is equivalent to the local time 12:00-13:00, the unfiltered mean
441 ergodic function of eddies in all possible scales in convective boundary layer cannot
442 converge to zero before filtering, i.e. cannot satisfy the condition of mean ergodic
443 theorem. That may be that eddies in all possible scales before filtering including the
444 local circulation in convective boundary layer. So we argue that, under general
445 situations, the eddies only below 10 min in the temporal scale or within 600-1200 m
446 in the spatial scale in ABL are the ergodic stationary random processes, but also the

447 turbulence including the eddies with all possible scales in ABL may belong to the
448 non-ergodic stationary random processes.

449 4.2.5 Relation between the ergodicity and local stability of different scale eddies

450 The corresponding eddy local stabilities z/L_c of eddies in different scales at different
451 time frames (see Table 1) show that the eddy local stabilities z/L_c of different scale
452 eddies are different, due to the fact that the temperature stratification in ABL has
453 different effect on the stability for different scale eddies. Even entirely contrary results
454 can occur. At the same time, the stratification that causes the large scale eddy to
455 ascend with buoyancy may cause the small scale eddy to descend. However, the
456 results in Figs. 1-3 show that the ergodicity is mainly related to the eddy scale, and its
457 relation with the atmospheric temperature stratification seems unimportance.

458 **4.3 Verification of autocorrelation ergodic theorem for different scale eddies**

459 In this section, Eqs. (7a) and (7b) are used to verify the autocorrelation ergodic
460 theorem. It is accordant with Sect. 4.2 that the turbulent eddies below 10 min in
461 temporal scale satisfy the mean ergodic condition in the various time frames, i.e., the
462 turbulent eddies below 10 min in temporal scale are at least strictly stationary random
463 processes or narrow stationary random processes whether in the nocturnal stable
464 boundary layer, or in the early neutral boundary layer and midday convective
465 boundary layer. Then we analyze further the different scale eddies that satisfy the
466 mean ergodic condition whether or not also satisfy the autocorrelation ergodic
467 condition, so as to verify atmospheric turbulence is whether narrow or wide stationary
468 random processes. The autocorrelation ergodic function of turbulence variable A
469 under the condition of truncated relaxation time $\tau_{i=n}$ is calculated according to the Eq.
470 (7a) to determine the variation of autocorrelation ergodic function $Er(A)$ with
471 relaxation time τ . As with the mean ergodic function $Ero(A)$, if the autocorrelation
472 ergodic function $Er(A)$ of eddies of 2 min, 3 min, 5 min, 10 min, 30 min and 60 min in
473 the temporal scale within the relaxation time $\tau_{i=n}$ is approximate to 0, then A shall be
474 deemed to be approximately ergodic; the more the autocorrelation ergodic function
475 deviates from 0, the worse the autocorrelation ergodicity becomes. Therefore, this
476 method can be used to judge approximatively whether the different scale eddies
477 satisfy the condition of autocorrelation ergodic theorem.

478 For example, Fig. 5 shows the variation of normalized autocorrelation ergodic
479 function $Ero(w)/u^*$ of the turbulent eddies of 2 min, 3 min, 5 min, 10 min, 30 min and

480 60 min in the temporal scale with relaxation time τ for the vertical velocity during the
481 time frames at 3:00-4:00, 7:00-8:00 and 13:00-14:00 (CST) respectively. Some basic
482 conclusions are drawn from Fig. 5 as following:

- 483 1. After comparing the Figs. 5a-c with the Figs. 1a-c, i.e., comparing the
484 dimensionless mean ergodic function $Ero(w)/u^*$ of vertical velocity with the
485 dimensionless autocorrelation ergodic function $Er(w)/u^*$, two basic characteristics
486 are very clear. First, the magnitudes of the dimensionless autocorrelation ergodic
487 function $Er(w)/u^*$, regardless of whether in the nocturnal stable boundary layer,
488 early neutral boundary layer or midday convective boundary layer, are all greatly
489 reduced. In Figs. 1a-c, the magnitudes of $Ero(w)/u^*$ are respectively 10^{-5} , 10^{-4} and
490 10^{-4} , and the magnitudes of $Er(w)/u^*$ are respectively 10^{-7} , 10^{-5} and 10^{-5} as shown in
491 Figs. 5a-c. The magnitudes of $Er(w)/u^*$ reduce by 1-2 magnitudes compared with
492 those of $Ero(w)/u^*$. Second, all autocorrelation ergodic functions $Er(w)/u^*$ of the
493 eddies of 30 min and 60 min in temporal scale, regardless of whether they are in
494 the stable boundary layer, natural boundary layer or convective boundary layer, are
495 all reduced and approximate to $Ero(w)/u^*$ of the eddies below 10 min in temporal
496 scale.
- 497 2. The above two basic characteristics imply that the autocorrelation ergodic function
498 $Er(w)/u^*$ of the stable boundary layer, neutral boundary layer or convective
499 boundary layer converges to 0 faster than the mean ergodic function $Ero(w)/u^*$; the
500 autocorrelation ergodic function of eddies of 30 min and 60 min in temporal scale
501 also converges to 0 and satisfies the condition of autocorrelation ergodic theorem,
502 except for the fact that the autocorrelation ergodic function $Er(w)/u^*$ of the eddies
503 below 10 min in temporal scale can converge to 0 and satisfy the condition of
504 autocorrelation ergodic theorem.
- 505 3. According to the autocorrelation ergodic function Eq. (7a), the eddies of 30 min, 60
506 min and below 10 min in the temporal scale, regardless of whether they are in the
507 stable boundary layer, neutral boundary layer or convective boundary layer, all
508 eddies can satisfy the condition of autocorrelation ergodic theorem. Therefore, in
509 general ABL's turbulence is the stationary random processes of autocorrelation
510 ergodicity.
- 511 4. The above results show that the eddies below 10 min in temporal scale in the
512 nocturnal stable boundary layer, early neutral boundary layer and midday

513 convective boundary layer can not only satisfy the condition of mean ergodic
514 theorem, but also they can also satisfy the condition of autocorrelation ergodic
515 theorem. Therefore, eddies below 10 min in the temporal scale are a wide ergodic
516 stationary random processes. Although the eddies of 30 min and 60 min in
517 temporal scale in the stable boundary layer, neutral boundary layer and convective
518 boundary layer can satisfy the condition of autocorrelation ergodic theorem, but
519 they cannot satisfy the condition of mean ergodic theorem. Therefore, eddies of 30
520 min and 60 min in the temporal scale are neither narrow ergodic stationary random
521 processes, nor wide ergodic stationary random processes.

522 **4.4 Ergodic theorem verification of different scale eddies for the multiple stations**

523 The basic principle of turbulence average is an ensemble average of the space, time
524 and state. Sections 4.2 and 4.3 verify the mean ergodic theorem and autocorrelation
525 ergodic theorem of atmospheric turbulence using field observational data, so that the
526 finite time average of a single station can be used to substitute for the ensemble
527 average. This section examines the ergodicity of different scale eddies according to
528 the observational data from CASES-99's center tower and six sub-sites (in all seven
529 stations). When the data are selected, it is considered that if the eddies are not evenly
530 distributed at the seven stations, then the observation results at the seven stations may
531 have originated from many eddies in the large scale. For this reason, the high
532 frequency variance spectrum above 0.1 Hz is compared firstly. Based on the
533 observational error, if the scatter of all high frequency variances does not exceed the
534 average by $\pm 10\%$, then it is assumed that the turbulence is evenly distributed at the
535 seven observation stations. And then, 17 datasets are chosen from among the
536 observed turbulence data from 5 to 30 October, and these data sets represent typical
537 strong turbulence at noon on the sunny day. As an example, the same method as
538 described in Sections 4.2 and 4.3 is used to respectively calculate variation of the
539 mean ergodic function and autocorrelation ergodic function with relaxation time τ for
540 the vertical velocity at 10:00-11:00 AM on 7 October. The time series composed of
541 the above data sets are performed band-pass filtering in 2 min, 3 min, 5 min, 10 min,
542 30 min and 60 min. The variations of mean ergodic function $E_{ro}(w)/u_*$ and
543 autocorrelation ergodic function $E_r(w)/u_*$ with relaxation time τ are analyzed for the
544 vertical velocity to test the ergodicity of different scale eddies for observation of the
545 multi-station. Fig. 6a shows variation of mean ergodic function $E_{ro}(w)/u_*$ with the

546 relaxation time τ for the vertical velocity, and Fig. 6b shows variation of
547 autocorrelation ergodic function $Er(w)/u^*$ with the relaxation time τ .

548 The results show ergodic characteristics of different scale eddies measured at the
549 multi-stations as following:

550 Fig. 6a shows that the mean ergodic function of eddies below 30 min in temporal
551 scale converges to 0 very well, except for the fact that the mean ergodic function of
552 eddies of 60 min in temporal scale clearly deviates upward from 0. Fig. 6b shows that
553 autocorrelation ergodic function of all different scale eddies including 60 min in
554 temporal scale, gradually converges to 0. Therefore, eddies below 30 min in temporal
555 scale measured at the multi-stations satisfy the conditions of both the mean and
556 autocorrelation ergodic theorem, while eddies of 60 min in temporal scale only
557 satisfies the condition of autocorrelation ergodic theorem, but cannot satisfy the
558 condition of mean ergodic theorem. These facts demonstrate that eddies below 30 min
559 in temporal scale are the wide ergodic stationary random processes for time series of
560 above data sets composed by the seven stations. This signifies that comparing of data
561 composed of the multiple stations with data from a single station, the eddy temporal
562 scale of wide ergodic stationary random processes is extended from below 10 min to
563 30 min. As analyzed above, if the eddies below 10 min in temporal scale are deemed
564 to be the turbulent eddies in the ABL with height about 1000 m, and the eddies of 30
565 min in the temporal scale, which is equivalent to that the space scale is greater than
566 2000 m, are deemed including eddy components of the local circulation in ABL, in
567 that way the multiple station observations can completely capture the local circulated
568 eddies, which space scale is greater than 2000 m.

569 **4.5 Average time problem of turbulent quantity averaging**

570 The atmospheric observations are impossible to repeat experiment exactly, must use
571 the ergodic hypothesis and replace ensemble averages with time averages. It arises a
572 problem how does determine the averaging time.

573 The analyses on the ergodicity of different scale eddies in above two sections
574 demonstrate that the eddies below 10 min in temporal scale as $\tau=30$ min in the stable
575 boundary layer, neutral boundary layer and convective boundary layer can not only
576 satisfy the mean ergodic theorem, but also can also satisfy the autocorrelation ergodic
577 theorem. That is to say, they are namely wide ergodic stationary random processes.
578 Therefore, a finite time average of 30 min within relaxation time τ can be used for

579 substituting for the ensemble average to calculate mean random variable Eq. (2).
580 However, the eddies of 30 min and 60 min in temporal scale in the stable boundary
581 layer and neutral boundary layer are only autocorrelation ergodic random processes,
582 neither narrow nor wide sense random processes. Therefore, when the finite time
583 average of 30 min can be used for substituting for the ensemble average to calculate
584 mean random variable Eq. (2), it may capture the eddies below 10 min in temporal
585 scale in stationary random processes, but cannot completely capture the eddies above
586 30 min in temporal scale. The above results signify that the turbulence average is
587 restricted not only by the mean ergodic theorem, but also is closely related to the scale
588 of turbulent eddy. In the observation performed using the eddy covariance technique,
589 the substitution of ensemble average with finite time average of 30 min inevitably
590 results in a high level of error, due to loss of low frequency component information
591 associating with the large-scale eddies. However, although eddies of 30 min and 60
592 min in temporal scale in convective boundary layer are not wide ergodic stationary
593 random processes, they are autocorrelation ergodic random processes. This may imply
594 that the mean random variable which is calculated with the finite time average in the
595 convective boundary layer to substitute for the ensemble average is often superior to
596 the results of the stable boundary layer and neutral boundary layer. Withal, the results
597 in the previous sections also show that the mean ergodic function of vertical velocity
598 may more easily converge to 0 than functions corresponding to the temperature and
599 humidity, i.e., the vertical velocity may more easily satisfy the condition of mean
600 ergodic theorem than the temperature and humidity. Therefore, in the observation
601 performed using the eddy covariance technique, the result of vertical velocity is often
602 superior to those of the temperature and humidity. In the previous section, the results
603 also point out that multi-station observation can completely capture eddies of the local
604 circumfluence in the ABL. Therefore, the multi-station observation is more likely to
605 satisfy the ergodic assumption, and its results are much closer to the true values. In
606 order to determine the averaging time, Oncley (1996) defined an Ogive function of
607 cumulative integral

$$608 \quad Og_{x,y}(f_0) = \int_{\infty}^{f_0} Co_{x,y}(f) df \quad (15)$$

609 where x and y are any two variables whose covariance is \overline{xy} , $Co_{xy}(f)$ is the
610 cospectrum of xy . If the Ogive function converges to a constant value at a frequency

611 $f=f_0$, which could be converted to an averaging time. Ogive function of $\overline{u'w'}$ is often
612 used to examine the minimal averaging time. As a comparison, here the variation of
613 Ogive functions of $\overline{w'^2}$ and $\overline{u'w'}$ with frequency at the height 3.08 m in NSPCE for
614 the three time frames is shown in Fig.7. The Fig.7 shows convergence frequency of
615 Ogive function for $\overline{w'^2}$ in the nighttime stable condition, morningtide neutral
616 boundary layer and midday convection boundary layer is respectively about at 0.01
617 Hz, 0.0001 Hz and 0.001 Hz. It is equivalent to the averaging times about 2 min, 160
618 min and 16 min. For $\overline{u'w'}$, it converges about at 0.001 Hz only in the midday
619 convection boundary layer to be equivalent to the averaging time about 16 min; it
620 seems no convergence in the nighttime stable and morningtide neutral boundary layer.
621 It is implied seemingly determining the averaging time has a bit difficult with the
622 Ogive function in the stable and neutral boundary layer. Fig.7 shows also that when
623 the frequency is lower than 0.0001Hz, Ogive functions $\overline{u'w'}$ ascend in the stable
624 boundary layer, but descend in the morningtide neutral boundary layer and midday
625 convection boundary layer. We must especially note that Ogive function is a
626 cumulative integral. So as Ogive function changes direction from ascending to
627 descending, it implies a possibility that there exists a superimposing of the negative
628 and positive momentum fluxes caused by a cross local circulation effect in nighttime
629 and midday. This cross local circulation in ABL may cause the low frequency effect
630 on the Ogive function. So that the local circulation in ABL may be an important cause
631 that Ogive fails to judge the averaging time. In this work, the choice of averaging time
632 with the ergodic theory seems superior to with the Ogive function.

633 **4.6 MOS of turbulent eddies in different scales and its relation with ergodicity**

634 Turbulent variance is a most basic characteristic quantity of the turbulence.
635 Turbulence velocity variance, which represents turbulence intensity, and the variance
636 of scalars, such as temperature and humidity, effectively describes the structural
637 characteristics of turbulence. In order to test MOS relation of the different scale
638 eddies with ergodicity, the vertical velocity and temperature data of NSPCE from 23
639 July to 13 September are used to determine the MOS relationship of variances of
640 vertical velocity and temperature for the different scale eddies, and to analyze its
641 relation with the ergodicity.

642 The MOS relation of vertical velocity variance as following:

643 $\phi_i(z/L) = c_1(1 - c_2 z/L)^{1/3}, \quad z/L < 0, \quad (16)$

644 $\phi_i(z/L) = c_1(1 + c_2 z/L)^{1/3}, \quad z/L > 0. \quad (17)$

645 Fig. 8 and 9 respectively shows the MOS relation curves of different scale eddies for
 646 the vertical velocity and temperature variances in NSPCE. The figures (a), (b) and (c)
 647 of Fig. 8 and 9 are respectively the similarity curve of eddies of 10 min, 30 min and
 648 60 min in the temporal scale. Table 2 shows the relevant parameters of fitting curve of
 649 MOS relation for the vertical velocity variance. The correlation coefficient and
 650 residual of fitting curve are respectively expressed with R and S .

651 Fig. 8 and Table 2 show that the parameters of fitting curve are greatly different,
 652 even if the fitting curve modality of MOS relation of the vertical velocity variance is
 653 the same for the eddies in different temporal scales. The correlation coefficients of
 654 MOS's fitting curve of the vertical velocity variance under the unstable stratification
 655 are large, but the correlation coefficients under the stable stratification are small.
 656 Under unstable stratification, the correlation coefficient of eddies of 10 min in the
 657 temporal scale reaches 0.97, while the residual is only 0.16; under the stable
 658 stratification, the correlation coefficient reduces to 0.76, and the residual increases to
 659 0.25. With the increase of eddy temporal scale from 10 min (Fig. 8a) to 30 min (Fig.
 660 8b) and 60 min (Fig. 8c), the correlation coefficients of MOS relation of the vertical
 661 velocity variance gradually reduce, and the residuals increase. The correlation
 662 coefficient in 60 min reaches a minimum; it is only 0.83 under the unstable
 663 stratification, and only 0.30 under the stable stratification.

664 The temperature variance is shown in Fig. 9. MOS's function to fit from eddies of
 665 10 min in the temporal scale under the unstable stratification is following:

666 $\phi_\theta(z/L_c) = 4.9(1 - 79.7 z/L_c)^{-1/3}. \quad (18)$

667 As shown in Fig. 9a, the correlation coefficient of fitting curve is 0.91 and residual is
 668 0.38. With increase of the eddy temporal scale, discreteness of MOS relation of the
 669 temperature variance is enlarged quickly to incur that the appropriate curve cannot be
 670 fitted.

671 The above results show that the discreteness of fitting curve of MOS relation for
 672 the turbulence variance is enlarged with the increase of eddy temporal scale for either
 673 the vertical velocity or temperature. The points of data during the stationary processes
 674 basically gather nearby the fitting curve of variance similarity relation, while all data

675 points during the non-stationary processes deviate significantly from the fitting curve.
676 However, the similarity of vertical velocity variance is superior to that of the
677 temperature variance. These results are consistent to the conclusions of testing
678 ergodicity for the different scale eddies described in Sections 4.2-4.4. The ergodicity
679 of the small-scale eddies is superior to that of the larger-scale eddies, and eddies of 10
680 min in the temporal scale have the best variance similarity function. These results also
681 signify that when eddies in the stationary random processes satisfy the ergodic
682 condition, then both the vertical velocity variance and temperature variance of eddies
683 in the different temporal scales comply with MOST very well; but, as for eddies with
684 poor ergodicity during non-stationary random processes, the variances deviate from
685 MOS relations.

686 **5 Conclusions**

687 From the above results, we can draw the below preliminary conclusions:

- 688 1. The turbulence in ABL is an eddy structure. When the temporal scale of turbulent
689 eddies in ABL is about 2 min, the corresponding spatial scale is about 120-240 m
690 to be equivalent to ASL's height; when the temporal scale of turbulent eddies in
691 ABL is about 10 min, the corresponding spatial scale is about 600-1200 m to be
692 equivalent to the ABL's height. For the eddies of larger temporal and spatial scale,
693 such as eddies of 30-60 min in the temporal scale, the corresponding spatial scale
694 is about 1800-3600 m to exceed the ABL's height.
- 695 2. For the atmospheric turbulent eddies below the ABL's scale, i.e. the eddies below
696 about 1000 m in the spatial scale and about 10 min in the temporal scale, the mean
697 ergodic function $Ero(A)$ and autocorrelation ergodic function $Er(A)$ converge to 0,
698 i.e., they can satisfy the conditions of mean and autocorrelation ergodic theorem.
699 However, for the atmospheric turbulent eddies above 2000-3000m in the spatial
700 scale and above 30-60 min in the temporal scale, the mean ergodic function doesn't
701 converge to 0, thus cannot satisfy the condition of mean ergodic theorem.
702 Therefore, the turbulent eddies below the ABL's scale belong to the wide ergodic
703 stationary random processes, but the turbulent eddies that are larger than ABL's
704 scale belong to the non-ergodic random processes, or even the non-stationary
705 random processes.
- 706 3. Due to above facts, when the stationary random process information of eddies
707 below 10 min in the temporal scale and below 1000 m of ABL's height in the

708 spatial scale can be captured, the atmospheric turbulence may satisfy the condition
709 of mean ergodic theorem. Therefore, an average of finite time can be used to
710 substitute for the ensemble average to calculate the mean of random variable as
711 measuring atmospheric turbulence with the eddy covariance technique. But for the
712 turbulence of eddies to be larger than 30 min in temporal scale, i.e., 2000 m in
713 spatial scale magnitude, it cannot satisfy the condition of mean ergodic theorem, so
714 that the eddy covariance technique cannot completely capture the information of
715 non-stationary random processes. This will inevitably cause a high level of error
716 due to the loss of low frequency component information associating with the
717 large-scale eddies when the average of finite time is used to substitute for the
718 ensemble average in the experiments.

719 4. Although the atmospheric temperature stratification has different effects on the
720 stability of eddies in the different scales, the ergodicity is mainly related to the
721 eddy local stability, and its relation with the stratification stability of ABL is not
722 significant.

723 5. The data series composed from seven stations compare with the observational data
724 from a single station. The results show that the temporal and spatial scale of eddies
725 to belong to the wide ergodic stationary random processes are extended from 10
726 min to below 30 min and from 1000 m to below 2000 m respectively. This signifies
727 that the ergodic assumption is more likely to be satisfied well with multi-station
728 observation, and observational results produced by the eddy covariance technique
729 are much closer to the true values when calculating the turbulence averages,
730 variances or fluxes.

731 6. If the ergodic conditions of stationary random processes are more effectively
732 satisfied, then the turbulence variances of eddies in the different temporal scales
733 can comply with MOST very well; however, the turbulence variances of the
734 non-ergodic random processes deviate from MOS relations.

735

736 **6 Discussions**

737 1. Galanti and Tsinober (2004) proved that the turbulence which was temporally
738 steady and spatially homogeneous is ergodic, but ‘partially turbulent flows’ such as
739 the mixed layer, wake flow, jet flow, flow around and boundary layer flow may be
740 non-ergodic turbulence. However, it has been proven through atmospheric
741 observational data that the turbulence ergodicity is related to the scale of turbulent

742 eddies. Since the large-scale eddies in ABL may be strongly influenced by the
743 boundary disturbance, thus belong to ‘partial turbulence’; however, since the
744 small-scale eddies in atmospheric turbulence may be not influenced by boundary
745 disturbance, may be temporally steady and spatially homogeneous turbulence. So
746 that the mean ergodic theorem and autocorrelation ergodic theorem are applicative
747 for turbulence eddies in the small scale in ABL, but the ergodic theorems aren’t
748 applicative for the large-scale eddies, i.e., the small-scale eddies in the ABL are
749 ergodic and the large-scale eddies exceeding the ABL’s scale are non-ergodic.

750 2. The eddy covariance technique for turbulence measurement is based on the ergodic
751 assumption. A lack of ergodicity related to the presence of large-scale eddy
752 transport can lead to a consider error of the flux measurement. This has already
753 been pointed out by Mauder et al. (2007) or Foken et al. (2011). Therefore, we
754 realize from the above conclusions that the large scale eddies that exceed ABL’s
755 height may include component of non-ergodic random processes. The eddy
756 covariance technique cannot capture the signals of large-scale eddies exceeded
757 ABL’s scale, thus resulting in the large error in the measurements of atmospheric
758 turbulent variance and covariance. MOST is developed under the condition of the
759 steady time and homogeneous surface. MOST’s conditions, steady time and
760 homogeneous underlying surface, are in line with the ergodic conditions, therefore
761 the turbulence variances, even the turbulent fluxes of eddies in different temporal
762 scales may comply with MOST very well, if the ergodic conditions of stationary
763 random processes are more effectively satisfied.

764 3. According to Kaimal and Wyngaard (1990), the atmospheric turbulence theory and
765 observation method were feasible and led to success under ideal conditions
766 including a short period, steady state and homogeneous underlying surface, and
767 through observation in the 1950s-1970s, but these conditions are rare in reality. In
768 the land surface processes and ecosystem, the turbulent flux observations in ASL
769 turn into a scientific issue in which commonly interest researchers in the fields of
770 atmospheric sciences, ecology, geography sciences, etc. These observations must
771 be implemented under conditions such as with complex terrain, heterogeneous
772 surface, long period and unsteady state. It is necessary that more neoteric
773 observational tools and theories will be applied with new perspectives in future
774 research.

- 775 4. It is successful that the banauasic ergodic theorem of stationary random processes is
776 introduced from the mathematics into atmospheric sciences. It undoubtedly
777 provides a profited tool for overcoming the challenges which encounter during the
778 modern measurements of atmospheric turbulent flow. At least it offers a promising
779 first step to diagnosticate directly the ergodic hypotheses for ASL's flows as a
780 criterion. And that the necessary and sufficient conditions of ergodic theorem can
781 introduce to the applicative scope of eddy covariance technique and MOST, and
782 seek potential reasons disable for using them in the ABL.
- 783 5. In the future, we shall keep up to study the ergodic problems for the atmospheric
784 turbulence measurements under the conditions of complex terrain, heterogeneous
785 surface and unsteady, long observational period, and to seek effective schemes. The
786 above results indicate the atmospheric turbulent eddies below the scale of ABL can
787 be captured by the eddy covariance technique and comply with MOST very well.
788 Perhaps MOST can be as the first order approximation to deal with the turbulence
789 of eddies below ABL's scale satisfying the ergodic theorems, then to compensate
790 the effects of eddies dissatisfying the ergodic theorems, which may be caused by
791 the advection, local circulation, low frequency effect, etc. under the complex
792 terrain, heterogeneous surface. For example, we developed a turbulent theory of
793 non-equilibrium thermodynamics (Hu, Y., 2007; Hu, Y., et al., 2009) to find the
794 coupling effects of vertical velocity, which is caused by the advection, local
795 circulation, and low frequency, on the vertical fluxes. The coupling effects of
796 vertical velocity may be as a scheme to compensate the effects of eddies
797 dissatisfying the ergodic theorems (Hu, Y., 2003; Chen, J., et al., 2007, 2013).
- 798 6. It is clear that such studies are preliminary, and many problems require further
799 research. The attestation of more field experiments is necessary.

800

801 *Acknowledgements.* This study is supported by the National Natural Science
802 Foundation of China under Granted Nos. 91025011, 91437103 and National Program
803 on Key Basic Research Project (2010CB951701-2). This work was strongly supported
804 by Heihe Upstream Watershed Ecology-Hydrology Experimental Research Station,
805 Chinese Academy of Sciences. We would like to express my sincere regards for their
806 support. And that we thank Dr. Gordon Maclean of NCAR for providing the detailed
807 CASES-99 data used in this study, and thank referees and editor very much for

808 heartfelt comments, discussions and marked errors.

809

810 References

811 Aubinet, M., Vesala, T., and Papale, D.: Eddy covariance, a practical guide to
812 measurement and data analysis, Springer, Dordrecht, Heidelberg, London, New
813 York, 438 pp., 2012.

814 Birkhoff, G. D.: Proof of the ergodic theorem, P. Natl. Acad. Sci. USA, 18, 656-660,
815 1931.

816 Boltzmann, L.: Analytischer beweis des zweiten Hauptsatzes der mechanischen
817 Wärmetheorie aus den Sätzen über das Gleichgewicht der lebendigen Kraft, Wiener
818 Berichte , 63, 712-732, in WAI, paper 20, 1871.

819 Chang, S. S. and Huynh, G. D.: Analysis of sonic anemometer data from the
820 CASES-99 field experiment. Army Research Laboratory, Adelphi, MD. 2002.

821 Chen, J., Hu, Y., and Zhang, L.: Principle of cross coupling between vertical heat
822 turbulent transport and vertical velocity and determination of cross coupling
823 coefficient, Adv. Atmos. Sci., 23, 639-648, 2007.

824 Chen, J., Hu, Y., Lu, S., and Yu, Ye.: Experimental demonstration of the coupling
825 effect of vertical velocity on latent heat flux, Sci. China. Ser. D-Earth Sci., 56,
826 1-9, 2013.

827 Eichinger, W. E., Parlange, M. B., Katul, G. G.: Lidar measurements of the
828 dimensionless humidity gradient in the unstable ASL, Lakshmi, V., Albertson, J.
829 and Schaake, J., Koster, R. D., Duan, Q., Land Surface Hydrology, Meteorology,
830 and Climate, American Geophysical Union, Washington, D. C. 7-13, 2001.

831 Ehrenfest, P., Ehrenfest-Afanassjewa, T.: The conceptual foundations of the statistical
832 approach in mechanics, Cornell University Press, New York, 114 pp., 1959.

833 Foken, T., Wichura, B.: Tools for quality assessment of surface-based flux

834 measurements. *Agric. For. Meteorol.*, 78, 83-105, 1996.

835 Foken, T., Göckede, M., Mauder, M., Mahrt, L., Amiro, B. D., and Munger, J. W.:
836 Post-field data quality control, in: *Handbook of micrometeorology: a guide for*
837 *surface flux measurement and analysis*, Lee, X., Massman, W. J., and Law, B.:
838 Kluwer, Dordrecht, 181-208, 2004.

839 Foken, T., Aubinet, M., Finnigan, J. J., Leclerc, M. Y., Mauder, M., Paw, U. K. T.:
840 Results of a panel discussion about the energy balance closure correction for
841 trace gases. *Bull. Am. Meteorol. Soc.*, 92, ES13-ES18, 2011.

842 Galanti, B. and Tsinober, A.: Is turbulence ergodic? *Phys. Lett. A*, 330, 173–18, 2004.

843 Higgins, C. W., Katul, G. G., Froidevaux, M., Simeonov, V. and Parlange, M. B.: Are
844 atmospheric surface layer flows ergodic? *Geophys. Res. Lett.*, 40, 3342-3346,
845 2013.

846 Hill, R. J.: Implications of Monin–Obukhov similarity theory for scalar quantities, *J.*
847 *Atmos. Sci.* 46, 2236–2244, 1989.

848 Hu, Y.: Convergence movement influence on the turbulent transportation in
849 atmospheric boundary layer, *Adv. Atmos. Sci.*, **20**, 794-798, 2003.

850 Hu, Y., Chen, J., Zuo, H.: Theorem of turbulent intensity and macroscopic mechanism
851 of the turbulence development, *Sci. China Ser. D-Earth Sci.*, **37**, 789-800, 2007.

852 Hu, Y., and Chen, J.: Nonequilibrium Thermodynamic Theory of Atmospheric
853 Turbulence, In: *Atmospheric Turbulence, Meteorological Modeling and*
854 *Aerodynamics*, Lang P., R. and Lombargo, F., S., Nova Science Publishers, New
855 York,, 59-110, 2010.

856 Kaimal, J. C. and Wyngaard, J. C.: The Kansas and Minnesota experiments,
857 *Bound.-Lay. Meteorol.*, 50, 31-47, 1990.

858 Kaimal, J. C. and Gaynor, J. E.: Another look at sonic thermometry, *Bound.-Lay.*

859 Meteorol., 56, 401–410, 1991.

860 Katul, G. G., Hsieh, C. I.: A note on the flux-variance similarity relationships for heat
861 and water vapor in the unstable atmospheric surface layer, *Bound.-Lay. Meteorol.*,
862 90, 327–338, 1999.

863 Katul, G., Cava, D., Poggi, D., Albertson, J., and Mahrt, L.: Stationarity, homogeneity,
864 and ergodicity in canopy turbulence, in: *Handbook of micrometeorology: a guide*
865 *for surface flux measurement and analysis*, Lee, X., Massman, W. J., and Law, B.:
866 Kluwer, Dordrecht, 161–180, 2004.

867 Krenkel, U.: *Ergodic theorems*, de Gruyter, Berlin, New York, 363 pp., 1985.

868 Lennaert van, V., Shigeo, K., and Genta, K.: Periodic motion representing isotropic
869 turbulence, *Fluid Dyn. Res.*, 38, 19–46, 2006.

870 Li, X., Hu, F., Pu, Y., Al-Jiboori, M. H., Hu, Z., and Hong, Z.: Identification of
871 coherent structures of turbulence at the atmospheric surface layer, *Adv. Atmos.*
872 *Sci.*, 19, 687-698, 2002.

873 Martano, P.: Estimation of surface roughness length and displacement height from
874 single-level sonic anemometer data, *J. Appl. Meteorol.*, 39, 708–715, 2000.

875 Mattingly, J. C.: On recent progress for the stochastic Navier Stokes equations,
876 *Journées équations aux dérivées partielles*, Univ. Nantes., Nantes., Exp. No. XI,
877 1-52, 2003.

878 Mauder, M., Desjardins, R. L., MacPherson, I.: Scale analysis of airborne flux
879 measurements over heterogeneous terrain in a boreal ecosystem. *J. Geophys.*
880 *Res.-ATMOS.*, 112, D13, 2007.

881 McMillen, R. T.: An eddy correlation technique with extended applicability to non
882 simple terrain, *Bound.-Lay. Meteorol.*, 43, 231-245, 1988.

883 Moore, C. J.: Frequency response corrections for eddy correlation systems,

884 Bound.-Lay. Meteorol., 37, 17-35, 1986.

885 Neumann, J. V.: Proof of the quasi-ergodic hypothesis, P. Natl. Acad. Sci. USA, 18,
886 70-82, 1932.

887 Oncley, S. P., Friehe, C. A., LaRue, J. C., Businger, J. A., Itsweire, E. C., Chang, S. S.:
888 Surface-layer fluxes, profiles, and turbulence measurements over uniform terrain
889 under near-neutral conditions, J. Atmos. Sci., 53, 1029-1044, 1996.

890 Padro, J.: An investigation of flux-variance methods and universal functions applied
891 to three land-use types in unstable conditions, Bound.-Lay. Meteorol., 66,
892 413–425, 1993.

893 Panofsky, H. A., Lenschow, D. H., and Wyngaard, J. C.: The characteristics of
894 turbulent velocity components in the surface layer under unstable conditions.
895 Bound.-Lay. Meteorol., 11, 355–361, 1977.

896 Papoulis, A. and Pillai, S. U.: Probability, random variables and stochastic processes.
897 McGraw Hill. New York. 666 pp., 1991.

898 Poulos, G. S., Blumen, W., Fritts, D. C., Lundquist, J. K., Sun, J., Burns, S. P., Nappo,
899 C., Banta, R., Newsom, R., Cuxart, J., Terradellas, E., and Balsley, Ben.: CASES-99:
900 A comprehensive investigation of the stable nocturnal boundary layer. Bull Am.
901 Meteorol. Soc., 83, 555–581, 2002.

902 Schotanus, P., Nieuwstadt, F. T. M., and de Bruin, H. A. R.: Temperature measurement
903 with a sonic anemometer and its application to heat and moisture fluxes,
904 Bound.-Lay. Meteorol., 26, 81–93, 1983.

905 Stull, R. B.: An introduction to boundary layer meteorology. Kluwer Academic Publ.
906 Dordrecht. 670 pp., 1988.

907 Uffink, J.: Boltzmann's work in statistical physics, Stanford encyclopedia of
908 philosophy, Edward, N. Z., 2004.

909 <http://plato.stanford.edu/entries/statphys-Boltzmann/>

910 Vickers, D., Mahrt, L.: Quality control and flux sampling problems for tower and
911 aircraft data. *J. Atmos. Ocean. Tech.*, 14, 512-526, 1997.

912 Webb, E. K., Pearman, G. I., and Leuning, R.: Correction of the flux measurements for
913 density effects due to heat and water vapor transfer, *Q. J. Roy. Meteor. Soc.*, 106,
914 85–100, 1980.

915 Wilczak, J. M., Oncley, S. P., Stage, S. A.: Sonic anemometer tilts correction
916 algorithms. *Bound.-Lay. Meteorol.*, 99, 127-150, 2001.

917 Wyngaard, J. C.: *Turbulence in the atmosphere, getting to know turbulence*,
918 Cambridge University Press, New York, 393 pp. 2010.

919 Zuo, H., Xiao X., Yang Q., Dong L., Chen J., Wang S.: On the atmospheric movement
920 and the imbalance of observed and calculated energy in the surface layer, *Sci. China*
921 *Ser. D-Earth Sci.*, 55, 1518-1532, 2012.

922

923

924

925

926

927

928

929

930

931

932

933

934

935

936

937

938

Table 1 Local Stability Parameter $(z-d)/L_c$ of the Eddies in Different Temporal Scales on 25 August

Time	3:00-4:00	7:00-8:00	14:00-15:00
Eddy scale			
≤ 2 min	0.59	0.52	-0.38
≤ 3 min	0.31	0.38	-0.44
≤ 5 min	0.28	0.16	-0.40
≤ 10 min	-0.01	0.15	-0.34
≤ 30 min	-0.04	-0.43	-0.27
≤ 60 min	-0.07	-1.29	-0.30

939

Table 2 Parameters of the Fitting Curve of MOS relation for Vertical Velocity Variance

	10 min		30 min		60 min	
	$z/L < 0$	$z/L > 0$	$z/L < 0$	$z/L > 0$	$z/L < 0$	$z/L > 0$
c_1	1.08	1.17	1.06	1.12	0.98	1.06
c_2	4.11	3.67	3.64	3.27	4.62	2.62
R	0.97	0.76	0.94	0.56	0.83	0.30
S	0.19	0.25	0.17	0.27	0.25	0.31

940

941

942

943

944

945

946

947

948

949

950

951

952

953

954

955

956

957

958

959

960

961

962

963

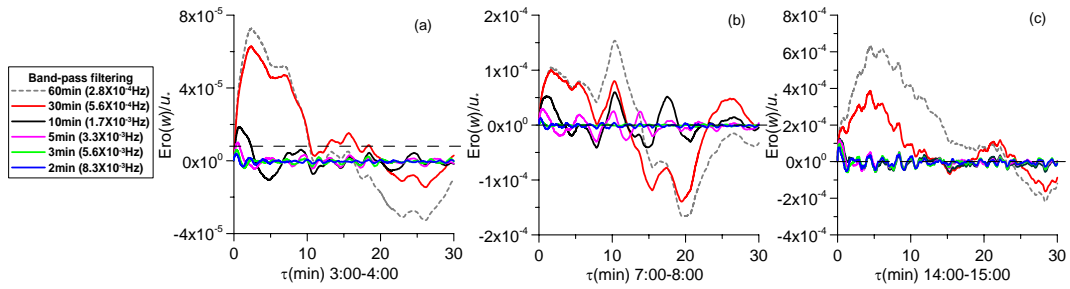


Fig. 1. Variation of mean ergodic function $Ero(w)$ of vertical velocity measured at the height 3.08 m in NSPCE with relaxation time for the different scale eddies after band-pass filtering. Panels (a), (b) and (c) are the respective results of the three time frames. If their mean ergodic function is more approximate to zero, then eddies in the corresponding temporal scale will more closely satisfy the ergodic conditions.

966

967

968

969

970

971

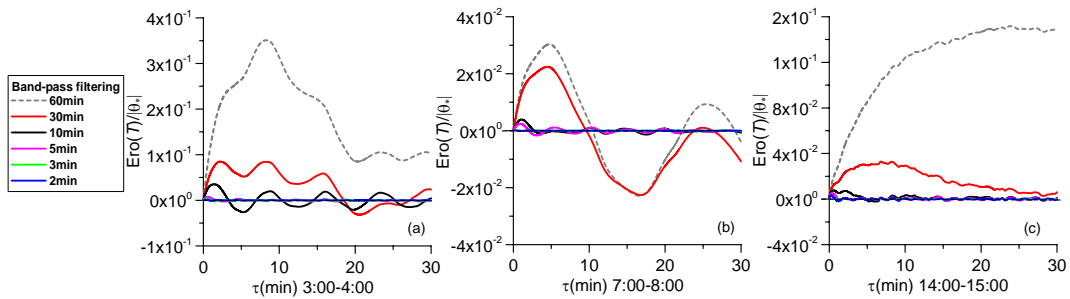


Fig. 2. Variation of mean ergodic function $Ero(T)$ of the different scale eddies of temperature with relaxation time (other conditions are similar to Fig. 2, and the same applies to the following figures).

974

975

976

977

978

979

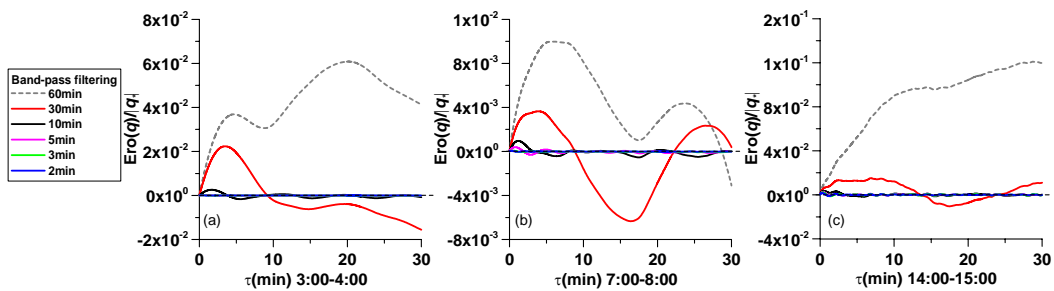


Fig. 3. Variation of mean ergodic function $Ero(q)$ of the different scale eddies of humidity with relaxation time.

981

982

983

984

985

986

987

988

989

990

991

992

993

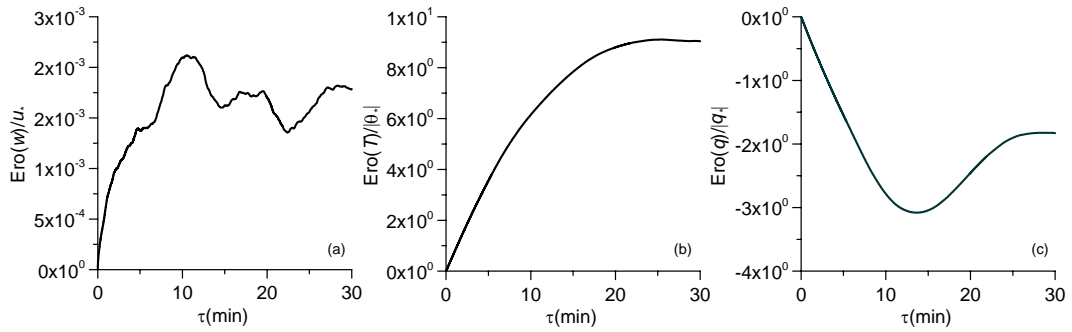
994

995

996

997

998



999 Fig. 4. Variation of mean ergodic function $Ero(w)$ of the vertical velocity (a), temperature (b) and specific humidity (c) before filtering during midday 14:00-15:00 (CST) in NSPCE with relaxation time τ .

1000

1001

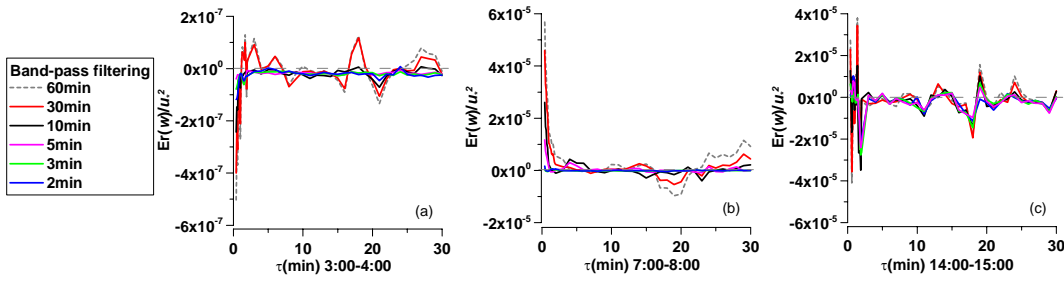
1002

1003

1004

1005

1006



1007 Fig. 5. Variation of the autocorrelation ergodic function of vertical velocity with relaxation time for different scale eddies.

1008

1009

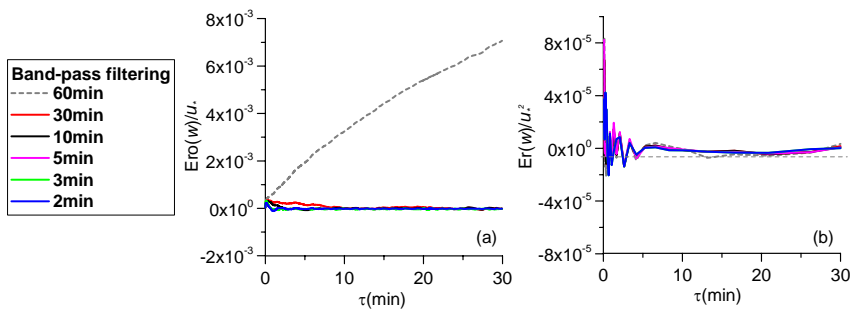
1010

1011

1012

1013

1014



1015 Fig. 6. Variation of mean ergodic function (a) and autocorrelation ergodic function (b) of the vertical velocity with relaxation time for the different scale eddies in CASES-99's seven stations.

1016

1017

1018

1019

1020

1021

1022

1023
 1024
 1025
 1026

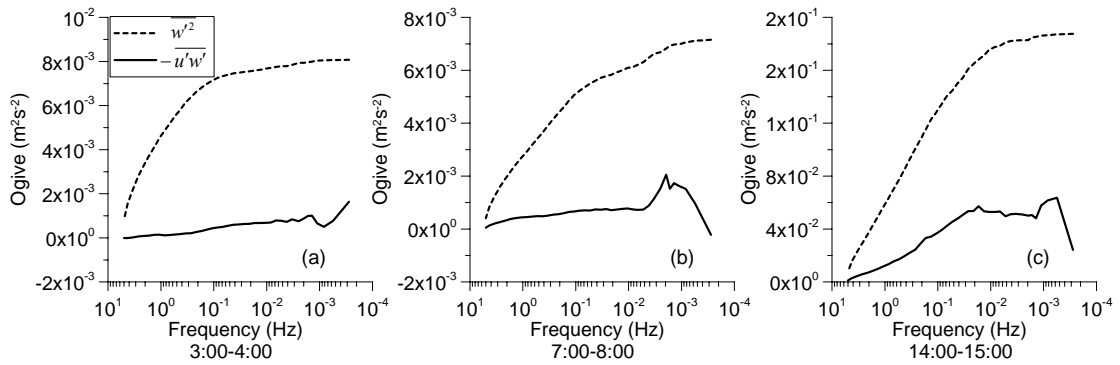


Fig. 7. Variation of Ogive functions of $\overline{w'^2}$ and $-\overline{u'w'}$ with frequency at the height 3.08 m in NSPCE for the three time frames.

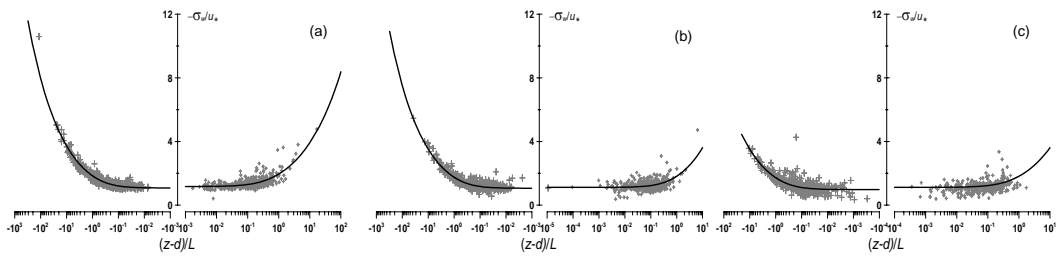


Figure 8. MOS relation of vertical velocity variances of the different scale eddies in NSPCE; Panels (a), (b) and (c) respectively represent the similarity of eddies of 10 min, 30 min and 60 min in the temporal scale.

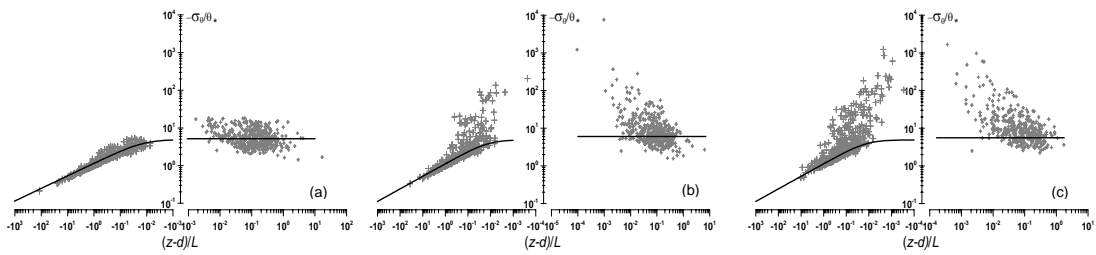


Figure 9. MOS relations of temperature variance of in different scale eddies of NSPCE; Panels (a), (b) and (c) respectively represent the similarity of the eddies of 10 min, 30 min and 60 min in the temporal scale.